PB-230 152

THE SURFACE SHEAR VISCOSITY OF MONOMOLECULAR FILMS

F. C. Goodrich

Clarkson College of Technology

Prepared for:

Environmental Protection Agency

1969

DISTRIBUTED BY:

NTIS

National Technical Information Service
U. S. DEPARTMENT OF COMMERCE
5285 Port Royal Road, Springfield Va. 22151

PB 230 152

FINAL REPORT

16050 DMZ

THE SURFACE SHEAR VISCOSITY OF MONOMOLECULAR FILMS

by

F. C. Goodrich
Department of Chemistry
Clarkson College of Technology
Potsdam, New York 13676

Reproduced by
NATIONAL TECHNICAL
INFORMATION SERVICE
U S Department of Commerce
Springfield VA 22151

THE SURFACE SHEAR VISCOSITY OF MONOMOLECULAR FILMS

1. Introduction

Attempts to measure rheological parameters at interfaces have long been hampered by an inadequate hydrodynamic analysis of the fluid motion involved. The customary procedure in almost all attempts to measure the surface shear viscosity of monomolecular films is to treat the fluid motion in the substrate and that in the film covered interface as though the two were independent of each other. While fully cognizant of the errors inherent in such an assumption (1), in the absence of a suitable theory experimentalists have had no alternative. The single exception to this state of affairs has been the use of the canal surface viscometer (2) for which a brief report on the flux through a canal floating at a water surface has been published by Kirkwood (3). This paper (without supporting mathematical analysis) depends upon the dangerous assumption that the monomolecular film is incompressible. Given the known high compressibility of many monomolecular films and the fact that the film must be forced through the canal under a gradient of surface pressure, this limitation of the theory is unsatisfactory. An additional drawback of the canal viscometer is the fact that the shear rate for steady flow through the canal, like that of its three dimensional analogue, the capillary or Poiseuille viscometer, is not constant, so that the instrument is not well suited to the study of non-Newtonian films.

The present study has been founded upon a careful mathematical analysis of the surface analogue of the Couette viscometer. Here the assumption of incompressibility of the film has also been used, but because counter rotating, coaxial rings or disks inserted into a fluid interface supporting a monomolecular film do not in the limit of slow rotation generate compressive stresses, the limitation is not a serious one. Furthermore, just as with the three dimensional Couette viscometer; the film entrapped between two counter rotating, coaxial rings, or between a rotating disk and an outer ring is subjected to nearly constant shear stress; and thus the instrument is well suited to the study of both Newtonian as well as non-Newtonian flow.

In the attached reprint (4) the basic mathematical analysis essential to an understanding of Couette flow at a free, fluid interface is presented. A grasp of the mathematical details contained in (4) is essential to an understanding of the theoretical parts of this report, but the numerical results will be presented in such a way as to be reasonably independent of the mathematical analysis.

2. The Disk Problem

Let a flat disk of radius a be inserted flush into a film covered fluid surface of infinite extent and infinite depth. Let it rotate slowly about its axis with constant angular velocity ω. Required is the angular component $v(r, z)$ of the fluid velocity vector at steady flow. Here r measures radial distance from the axis of the disk and z measures depth below the plane surface of the fluid (by convention z is taken negative in the interior of the liquid substrate).

It is shown in (4) that the solution of this problem is

$$v/\omega a = \int_0^\infty f(y)\, e^{yz}\, J_1(yr)\, dy \qquad (1)$$

in which J_1 is the Bessel function of order 1 and $f(y)$ is a linear combination of Bessel functions of order $J_{n+0.1}$.

$$f(y) = 2a(ay)^{-1.1} \sum_1^N c_n J_{n+0.1}(ay) \qquad (2)$$

The coefficients c_n in this linear combination were determined by a variation method whose accuracy improves as the number of terms N increases. For a monolayer covered interface of low surface viscosity our calculations were based upon N = 30, while for higher surface viscosities the choice N = 20 was adequate. The results depend upon the value of the dimensionless parameter $\lambda = \eta/\mu a$ where η is the surface viscosity of the monomolecular film (units g sec^{-1}) and μ is the conventional shear viscosity of the substrate (units g $sec^{-1} cm^{-1}$). Tables of coefficients c_n for selected values of λ are given in Appendix I.

When (2) is substituted into (1) and $z = 0$, we obtain velocity profiles $v(r, 0)$ for fluid flow in the monomolecular film. The results take a different form depending upon whether or not $r < a$ or $r > a$, i.e., whether or not we are interested in the fluid flow immediately beneath the rotating disk, or whether we are interested in the flow in the free, film covered interface. Because the integral (1) possesses a discontinuous derivative dv/dr at $r = a$, the computing formulas for the two cases will be different. In the former case $r < a$, the surface velocity profile beneath the disk is quite simply

$$v(r, 0) = \omega r, \tag{3}$$

meaning that there is no slip at the liquid/disk boundary. In the latter case $r > a$,

$$v(r, 0)/\omega a = 2^{-0.1} \sum_{1}^{N} c_n \frac{\Gamma(\frac{1}{2}n + 1/2)}{\Gamma(n + 1.1)\,\Gamma(3/2 - \frac{1}{2}n)} (\frac{a}{r})^n \tag{4}$$

$$\times F(\tfrac{1}{2}n + 1/2,\ \tfrac{1}{2}n - 1/2,\ n + 1.1,\ a^2/r^2)$$

in which $\Gamma(z)$ is the gamma function and $F(\alpha, \beta, \gamma, z)$ is the hypergeometric function. Some surface velocity profiles calculated from this formula are drawn in figure 1. More will be found in figure 4 of reference 4.

We have compared the predictions of formula (4) with the velocity profiles calculated from the two exactly known results when $\lambda = 0$ (zero surface viscosity) and $\lambda \longrightarrow \infty$ (infinite surface viscosity). These exactly known profiles are

$$v(r, 0)/\omega a = \frac{2}{\pi}\left[\frac{r}{a}\arcsin\frac{a}{r} - (1 - a^2/r^2)^{1/2}\right] \tag{5}$$

when $\lambda = 0$ and

$$v(r, 0)/\omega a = a/r \tag{6}$$

when $\lambda \longrightarrow \infty$. Profiles calculated from (4) in these two extreme cases agree with formulas (5) and (6) to within a maximum error of 1% for all values of r/a between 0 and 3.

3. The Torque on a Rotating Disk

In order to translate these results into predictions useful to the interpretation of experiments, it is convenient to compute the total torque exerted on the rotating disk by the combination of surface and bulk phase stresses which act upon it. At the rim of the disk the torque due exclusively to the viscosity of the monomolecular film may by standard hydrodynamic methods be shown to be

$$\text{Film torque} = 2\pi a^2 \eta \left[\frac{\partial v}{\partial r} - \frac{v}{r}\right]_{\substack{r = a \\ z = 0}} \tag{7}$$

In a similar way the torque exerted upon the base of the disk by the bulk substrate is

$$\text{Substrate torque} = -2\pi\mu \int_0^a r^2 \, (\partial v/\partial z)_{z = 0} \, dr \tag{8}$$

and the total torque measured by the experimenter will be the sum of these two contributions.

Let us consider the film torque (7) first. The most difficult part of the computation lies in the calculation of the derivative $\partial v/\partial r$ at the point $r = a$, for the reader will recall that $\partial v/\partial r$ is discontinuous at this point, so that what is required is the limiting value of $\partial v/\partial r$ as $r \longrightarrow a$ from above. Analytical differentiation of formula (4) will not work, for this variation form, while an accurate representation of v, is nevertheless no more than a finite harmonic analysis of the true velocity function, and the inability of such forms to yield derivatives at discontinuities by formal term by term differentiation is well known. We are instead required to differentiate the numerical data calculated from (4), and this poses severe problems (particularly at low surface viscosities) because of the

steeply rising nature of the velocity profile. Our results were eventually calculated by numerical differentiation of r data tabulated as a function of v, which is to say that we calculated dr/dv rather than dv/dr and then took the reciprocal. The ordinary numerical differentiation routines based upon the Lagrangian interpolation formula proved unsatisfactory, and our final results were computed by the Chebychev Polynomial method (5).

With the accumulation of a large number of derivatives dr/dv at r = a, we next expressed these derivatives as least squares polynomials in λ. For $0 \leq \lambda \leq 1$ the form of the polynomial chosen was

$$-\omega \left(\frac{dr}{dv}\right)_{r=a} = \sqrt{\lambda} \sum_{o}^{4} b_n \lambda^n \tag{9}$$

while for $\lambda > 1$ we used

$$-\omega \left(\frac{dr}{dv}\right)_{r=a} = 1 + \sum_{1}^{3} b_n \lambda^{-n} \tag{10}$$

A table of the coefficients b_n together with their range of validity in λ is listed in Appendix II. They reproduced the numerically computed derivatives $\omega (dr/dv)_{r=a}$ to within an accuracy of 1%.

To compute from (7) the film contribution to the total torque, we next used the reciprocals of derivatives calculated from (9) and (10) together with the known boundary condition at the rim of the disk, $v(a, 0)/a = \omega$. Expressed in dimensionless units, the film torque (7) is

$$\frac{\text{Film torque}}{\omega \mu a^3} = -2\pi\lambda \left[1 - \omega^{-1} \left(\frac{dv}{dr}\right)_{r=a}\right] \tag{11}$$

and the torque exerted by the experimenter on the disk to maintain its steady rotation will have a contribution which is equal in magnitude to (11) but opposite in sign.

A plot of the positive, right hand side of (11) in the low surface viscosity region is drawn in figure 2. For comparison purposes there is also drawn in figure 2 a plot of the "naive" film torque contribution which has been assumed by previous workers in surface viscosity. This plot is a result of assuming that the film and substrate flows are independent of each other, and has the practical effect in (11) of setting on the right hand side $\omega^{-1} \left(\frac{dv}{dr}\right)_{r=a} = -1$. This is actually the limiting theoretical value of this quantity as $\lambda \longrightarrow \infty$, so that at high surface viscosities $\lambda \gg 1$ the naive approach is satisfactory; but the assumption is evidently grossly in error at low and moderate surface viscosities.

I now turn to a consideration of the torque exerted by the substrate on the base of the rotating disk. Formal differentiation of (1) followed by substitution into (8) leads to

$$\text{Substrate torque} = -2\pi\omega\mu a \int_0^\infty y f(y)\,dy \int_0^a r^2 J_1(yr)\,dr$$
$$= -2\pi\omega\mu a^3 \int_0^\infty f(y)\, J_2(ya)\,dy \qquad (12)$$

in which J_2 is the Bessel function of order 2. Before substituting into (12) the variation form (2), it is illuminating to use the exactly known results (reference 4)

$$f(y) = 2(2a/\pi y)^{1/2} J_{3/2}(ay) \quad \ldots \text{ when } \lambda = 0$$

$$f(y) = 2\, y^{-1} J_1(ay) \quad \ldots \text{ when } \lambda = \infty.$$

In the former case I find from (12) the dimensionless quantities

$$-\frac{\text{Substrate torque}}{\omega\mu a^3} = 16/3 = 5.333 \text{ (zero surface viscosity)}$$

$$-\frac{\text{Substrate torque}}{\omega\mu a^3} = 8/3 = 2.667 \text{ (infinite surface viscosity)}$$

The presence of a highly viscous surface film thus modifies the torque on the base of the rotating disk, lowering it by a factor 1/2 from what is measured on a film free interface. In all previous work involving Couette surface viscometry, this lowering of the viscous traction on the rotating disk has been ignored. The implication is that at intermediate surface viscosities the substrate contribution to the total torque will be lowered by an intermediate factor.

For general values of the surface viscosity, we substitute (2) into (12) and integrate. The result is

$$\frac{\text{Substrate torque}}{\omega \mu a^3} = -2^{-0.9}\Gamma(1.1)\left\{c_2 \frac{\pi}{\Gamma(1.1)\Gamma(3.1)} + \sum_{\text{odd}} c_n (-1)^{(1/2)(n+1)} \frac{\Gamma(\frac{1}{2}n + 1)\Gamma(\frac{1}{2}n - 1)}{\Gamma(\frac{1}{2}n + 0.1)\Gamma(\frac{1}{2}n + 2.1)}\right\} \tag{13}$$

The notation $\sum_{\text{odd}}$ means that the sum is taken over odd values of n only. Using the c_n values listed in Appendix I, the positive right hand side of (13) (which is the torque exerted by the experimenter to maintain the disk in steady rotation) has been computed for selected values of the dimensionless surface viscosity λ, and the result is figure (3). It will be observed that at low surface viscosity, the substrate torque falls very rapidly with increasing λ, and then more slowly towards its asymptotic value of 8/3.

By summing the contributions (11) and (13) we have the total torque exerted on the disk by the combined action of the monomolecular film and the viscous drag of the substrate. A table of this total torque divided by $\omega \mu a^3$ together with the separate film and substrate contributions is given in Appendix III. Also tabulated is the excess torque = (total torque/$\omega\mu a^3$) - 16/3, which in dimensionless units is the difference between the total torque and that obtained for the film free interface. It is this last column which should be of most direct interest in the interpretation of experimental data, for the usual procedure in the laboratory has been to observe

the torque at a film free interface and then to compare it with the torque at the film covered interface. The excess torque is plotted in figure (4).

The "naive" approach which has been used by all experimentalists in Couette surface viscometry to date is to assume that the dimensionless substrate torque remains constant at 16/3 and that the dimensionless excess torque is identical with a film torque set equal to $4\pi\lambda$. A plot of this "naive" assumption is included in figure (4). In the low surface viscosity region it is seen to be seriously in error.

4. Discussion

The most unexpected feature of figure (4) is the prediction of a minimum in the plot of excess torque against surface viscosity, and indeed the fact that the excess torque can be negative. Translated into experimental terms, this means that if the excess torque is measured for a monolayer at a series of surface concentrations starting at infinite dilution, the excess torque will at first be negative, pass through a minimum while still at very low surface viscosities, and then rise again, passing through zero in the neighborhood of $\lambda = \eta/\mu a = 0.013$. Taking the substrate to be water with a viscosity $\mu = 0.01$ g sec^{-1} cm^{-1} and using a = 2 cm for the radius of the disk, the region of negative excess torque should occur for $\eta < 3 \times 10^{-4}$ g sec^{-1}. Surface viscosities of this order of magnitude and lower have been reported (6), although because they were calculated from an incorrect theory these figures must be accepted with reserve. In any case, no one has yet reported a negative excess torque in any experiment involving surface viscosity, and the search for such values poses an interesting experimental challenge.

The physical explanation of the minimum lies in the fact that the substrate torque is rapidly reduced by the presence of the monolayer, more rapidly than the concommitant increase in the film torque, so that as a result the total torque is lowered. In a very real sense, therefore, a dilute monolayer can "lubricate" the motion of a shallow object floating at an interface.

The perceptive reader will notice that the details of the minimum are not clearly shown in figure 4. The reason is that our numerical program, while accurate at all but the lowest surface viscosities, becomes unreliable in this region. We

have observed this in a tendency of the calculated points of the excess torque plot to scatter as the number of terms in the variation function (2) is varied from N = 20 to N = 30. In principle the accuracy could be improved by making N even larger, and while feasible from the point of view of machine time (4 minutes on the IBM 360 computer for each point at N = 30), the round off error becomes so severe that even in double precision arithmetic the results are not to be trusted. The basic theoretical difficulty lies in a singularity in the original integral equation upon which all of these results are based (see reference 4), and the inability of finite harmonic analysis to represent such singularities accurately.

Because of the failure of our finite variation routine in the ultra low surface viscosity region, I have spent a considerable amount of time over the past three years in seeking a perturbation expansion of the velocity field $v(r, z)$ as a power series in λ. This is the conventional perturbation approach, but all such attempts have foundered upon the fact that the coefficients in the perturbation series have contained divergent integrals. Only recently has it been possible to construct a non conventional perturbation method which gives promise of removing this difficulty. The method depends upon a rigorous treatment of the above mentioned singularity inherent in our integral equation. In any case, it has not yet been reduced to numerical results, and will thus not be further discussed.

5. The Disk-Ring Problem

A hydrodynamic analysis of the disk problem was a necessary preliminary to study of the more complicated disk-ring problem. Here the rotating disk inserted into the surface of an infinite mass of fluid is supplemented by a ring of larger radius b coaxial with the disk and maintained stationary by the experimenter. The idea here is to use the rotating disk to generate a hydrodynamic torque on the ring, a torque which is opposed by the experimental apparatus. In the following analysis I shall suppose that the ring is infinitely thin, making a knife edge contact to zero depth with the fluid surface. Because I wish to hold the mathematical details to a minimum, I must presume the reader to be thoroughly familiar with the procedures described in reference (4).

Equation (1) is still a valid representation of the velocity field, but because of the presence of the stationary ring, the function f(y) is different. At z = 0, the boundary conditions over the surface of the fluid require

$$\int_0^\infty f(y)\, J_1(ry)\, dy = r/a \qquad ; \quad r \le a \tag{14}$$

$$\int_0^\infty (\mu y + \eta y^2)\, f(y)\, J_1(ry)\, dy = 0 \qquad ; \quad a < r < b \tag{15}$$

$$\int_0^\infty f(y)\, J_1(by)\, dy = 0 \tag{16}$$

$$\int_0^\infty (\mu y + \eta y^2)\, f(y)\, J_1(ry)\, dy = 0 \qquad ; \quad r > b \tag{17}$$

In words, equation (14) is the condition of no slip between the base of the rotating disk and the fluid; (15) and (17) are the condition that over the free (monolayer) covered surface of the liquid, whether it be in the annulus between the disk and the ring or on the further side of the ring, the combination of monolayer shear stress plus bulk fluid phase shear stress shall sum to zero; and (16) requires that at r = b (the ring radius), the velocity field must be zero. The procedures of reference (4) will now be introduced. Multiply (14) by r and differentiate with respect to r.

$$a \int_0^\infty y f(y)\, J_0(yr)\, dy = 2; \quad r \le a \tag{18}$$

Now integrate (15) with respect to r from some r > a to b.

$$\int_0^\infty (\mu y + \eta y^2)\, f(y)\, dy \int_r^b J_1(ry)\, dr$$

$$= \int_0^\infty (\mu y + \eta y^2) f(y)\, dy \left[\int_r^\infty J_1 (ry)\, dr - \int_b^\infty J_1 (ry)\, dr \right]$$

$$= \int_0^\infty (\mu + \eta y) f(y) [J_o (ry) - J_o (by)]\, dy = 0$$

or $$\int_0^\infty (1 + \lambda ay) f(y) J_o (ry)\, dy = \int_0^\infty (1 + \lambda ay) f(y) J_o (by)\, dy$$

$$= \text{constant independent of } r \text{ for } a < r < b.$$

Here as usual $\lambda = \eta / \mu a$ is the dimensionless surface viscosity. This last equation may be rearranged to

$$a \int_0^\infty y f(y) J_o (ry)\, dy = A - \frac{1}{\lambda} \int_0^\infty f(y) J_o (ry)\, dy \qquad (19)$$

for $a < r < b$,

in which A is an undetermined constant.

Finally I integrate (17) from $r > b$ to ∞.

$$\int_0^\infty (1 + \lambda ay) f(y) J_o (ry)\, dy = 0$$

and rearrange to

$$a \int_0^\infty y f(y) J_o (ry)\, dy = - \frac{1}{\lambda} \int_0^\infty f(y) J_o (ry)\, dy \qquad (20)$$

for $r > b$

A special case of great interest is the limit $\lambda \longrightarrow \infty$ (infinite surface viscosity). By an examination of equations (18) through (20) it will be observed that they simplify to

$$a\int_0^\infty yf(y)\,J_o(ry)\,dy = 2 \quad \text{for } r \le a$$

$$= A \quad \text{for } a < r < b$$

$$= 0 \quad \text{for } r > b$$

The solution for f(y) may in this special case be readily obtained by the Hankel inversion theorem. The method is familiar, and I quote only the result.

$$f(y) = (2 - A)\,y^{-1} J_1(ay) + (Ab/a)\,y^{-1} J_1(by) \tag{21}$$

There remains the undetermined constant A, but this may be fixed by use of equation (16). When this is done I find

$$f(y) = 2\frac{a\,b^2}{b^2 - a^2}\left[(ay)^{-1} J_1(ay) - (by)^{-1} J_1(by)\right] \tag{22}$$

whence upon insertion into equation (1) we have for the velocity profile in the interface z = 0,

$$v(r,0)/\omega a = r/a \qquad \text{for } r \le a$$

$$v(r,0)/\omega a = \frac{ab}{b^2 - a^2}\left(\frac{b}{r} - \frac{r}{b}\right) \qquad \text{for } a < r < b \tag{23}$$

$$v(r,0) = 0 \qquad \text{for } r \ge b.$$

This profile is identical with what would be obtained by an initial assumption that the substrate played no role in determining the surface motion and then applying to the monomolecular film the ordinary equations of fluid dynamics appropriate to two dimensional flow. As with the rotating disk alone, however, the assumption is valid only in the limit $\lambda \longrightarrow \infty$.

In the general case when λ is finite, I apply the Hankel inversion theorem to the right hand sides of equations (18) through (20). After some rearrangement the result may be written as an integral equation in the unknown function f(y):

$$(1 + 1/\lambda a y)\, f(y) = w(y) + (1/\lambda a) \int_0^\infty K(y,\xi)\, f(\xi)\, d\xi \tag{24}$$

in which w(y) is the right hand side of (21) and

$$K(y,\xi) = K(\xi,y) = \int_0^\infty r\, J_0(ry)\, J_0(r\xi)\, dr$$

$$= \frac{a\xi\, J_1(a\xi)\, J_0(ay) - ay\, J_1(ay)\, J_0(a\xi)}{\xi^2 - y^2} \tag{25}$$

The constant A which occurs in w(y) is still undetermined, but after the solution of (24) for general values of A, this constant may be fixed by an appeal to equation (16).

The reader will recall from a perusal of reference (4) that a rather similar integral equation occurs in the rotating disk problem. Because I was unable to obtain an analytic solution for general values of λ in that case, it will come as no surprise to learn that I have been equally unsuccessful in the more complicated disk-ring problem represented by equation (24). The variation formalism introduced in the disk problem, however, is equally applicable here, although the computational details turn out to be far more complex.

A straightforward application of the calculus of variations shows that a solution f(y) of (24) gives a stationary value to the integral

$$\int_0^\infty \left[(1 + 1/\lambda y^2 a^2)\, f^2(y) - 2w(y)\, f(y) \right] dy$$

$$- (1/\lambda a) \int_0^\infty \int_0^\infty K(y,\xi)\, f(y)\, f(\xi)\, dy d\xi \tag{26}$$

$$= \text{stationary}$$

and by substituting into (26) the finite variation form

$$f(y) = (a/y)^{1/2} \left\{ c_1 J_{3/2}(ay) + c_2 J_{3/2}(by) + c_3 J_{5/2}(ay) + c_4 J_{5/2}(by) + \ldots \right\} \qquad (27)$$

the c's may be chosen to make (26) stationary. It turns out that all of the required integrals may be computed from known properties of the Bessel functions. The details are analogous to those used in reference (4), although exceedingly more complicated. An extra difficulty is the determination of the constant A so as to satisfy the ring boundary condition, equation (16); but I shall pass over a description of how this is done with the remark that instead of N linear variation coefficients c_n to be determined from (26) and (27), there are actually N + 1, with A as the extra coefficient.

A typical surface velocity profile computed from our program is given in figure (5) in which b has been set equal to 3a, meaning that the annulus of monolayer between the disk and the ring has a breadth equal to twice the disk radius. We are at the present time generating other machine computed profiles for narrower annuli in the expectation of using them in the construction of torque tables as was discussed above in the disk problem.

5. The Ring Problem

If the disk is removed from the problem discussed in section 4, there remains only a ring contact of the apparatus with the monomolecular layer, and if we give the ring a steady angular velocity ω, we have the problem of analyzing the motion mathematically. This problem gives promise of being soluable for general values of λ to a higher degree of approximation than has been the case for any of the problems so far discussed, for it is the only problem in which I have been able to dispense with the variation formalism. The velocity profile for knife edge ring contact with the interface is a Green's function for Couette surface viscometry in the sense that in principle, solutions to all problems involving concentric rotating

rings and disks can be constructed as linear combinations of the Green's function. Whether such a program can be pushed to numerical fruitfulness is not known at the present time.

Let us assign the ring a radius a (this radius was called b in section 4). Then at steady motion the velocity distribution is described by equation (1) and we impose boundary conditions at z = 0

$$\int_0^\infty (\mu y + \eta y^2)\, f(y)\, J_1(ry)\, dy = 0 \quad ; \quad r < a$$

$$\int_0^\infty f(y)\, J_1(ay)\, dy = 1 \quad ; \quad r = a \qquad (28)$$

$$\int_0^\infty (\mu y + \eta y^2)\, f(y)\, J_1(ry)\, dy = 0 \quad ; \quad r > a$$

The reader should compare these boundary conditions with equations (15) through (17). They express the facts that over the free surface of the film covered interface the surface shear stresses are exactly balanced by the bulk phase shear stresses, while at those points where the ring makes contact with the interface, $v(a, 0)/\omega a = 1$.

A casual examination of equations (28) shows that the integral

$$\int_0^\infty (\mu y + \eta y^2)\, f(y)\, J_1(ry)\, dy$$

vanishes everywhere except possibly at r = a. If we apply the Hankel inversion theorem to this situation, this suggests that the Hankel inversion operator acts upon a function which is zero everywhere except at r = a, at which point it becomes infinite. These are the properties of the Dirac delta function $\delta(r-a)$, so that formally

$$(\mu + \eta y)\, f(y) = \int_0^\infty r\, \delta(r-a)\, J_1(ry)\, dr = aJ_1(ay)$$

The implied form of f(y) is thus

$$f(y) = Aa\,(1 + \lambda ay)^{-1} J_1(ay) \tag{29}$$

in which as usual $\lambda = \eta / \mu a$ and A is the intensity or "amplitude" of the Dirac function. As a practical matter, A must be chosen so as to satisfy the second of equations (28):

$$Aa \int_0^\infty \frac{J_1(ay)\, J_1(ay)}{1 + \lambda\, ay}\, dy = 1$$

$$\text{or} \quad A^{-1} = \int_0^\infty \frac{J_1^2(x)}{1 + \lambda x}\, dx \tag{30}$$

This is the only problem in Couette surface viscometry for which I have been able to obtain an exact solution for f(y) for all values of λ.

The two extreme cases of $\lambda \longrightarrow \infty$ and $\lambda \longrightarrow 0$ are of special interest. In the former we obtain

$$f(y) = 2\, y^{-1} J_1(ay)$$

whence

$$v(r,0)/\omega a = r/a \;;\; r \leq a$$

$$v(r,0)/\omega a = a/r \;;\; r > a$$

This is identical with the solution to the problem of the rotating disk at infinite surface viscosity (see equation (6)), whence we conclude that a highly viscous monolayer confined by a rotating ring will rotate with the ring as a rigid body.

The limit of zero surface viscosity is a bit more subtle, for upon examination of (30) it appears that $A \longrightarrow 0$ as $\lambda \longrightarrow 0$, which means that the velocity distribution must also converge towards zero everywhere except at the knife edge contact $r = a$. I interpret this to mean that an infinitely thin ring is incapable of setting a liquid into motion in the absence of any surface viscosity. Confirmatory evidence that this is the correct interpretation is emerging from our machine programs on the disk-ring problem, for at low surface viscosities the perturbation of the velocity profile by the ring becomes progressively smaller, and the whole profile approaches that of the undisturbed rotating disk profile except in the immediate neighborhood of the ring.

These facts suggest that an alternative approach to the disk-ring problem is to use our machine output for the disk problem and then to superpose upon these velocity profiles just enough of a ring profile so as to satisfy the boundary condition $v(r, 0) = 0$ when $r =$ the ring radius. Essential to the success of this method would be the calculation of ring profiles obtained by the substitution of (29) into (1):

$$v(r, 0)/\omega a = Aa \int_0^\infty (1 + \lambda ay)^{-1} J_1 (ay) J_1 (ry)\, dy \qquad (31)$$

Such profiles represent the Green's function for surface Couette Viscometry. At the present time, however, we have no results to report concerning the computation of the integral (31).

6. Experimental Program

The experimental portion of our research program has been slow to yield results, and the design of the equipment is still undergoing minor modifications. The heart of the apparatus (figure 6) is a ring suspended from the moving coil of a sensitive galvanometer. The edge of the ring which makes contact with the monolayer covered interface is constructed from teflon ground to a knife edge. Coaxial with the ring and interior to it is a rotating teflon disk. The basic idea here is to generate a hydrodynamic torque on the ring by means of the rotating disk and then to apply an

equal but opposite electromagnetic torque by running current through the galvanometer, so that the current reading is a measure of the hydrodynamic torque. While this design is successful for high surface viscosities, it has not yielded reliable results in the low surface viscosity region; for any slight departure of the ring and the disk from being exactly coaxial produces unacceptably large oscillations in the current reading. When the monolayer possesses a high surface viscosity, these oscillations are effectively damped, but at low surface viscosities the ring apparently swings slightly away from its coaxial position, and this erratic motion vitiates the reading. We have been able to reduce the oscillation by increasing the mass of the ring, but this also has the inevitable result of reducing the sensitivity of the apparatus.

The apparatus is calibrated by removing the ring from the galvanometer coil and replacing it by a glass cylinder which is inserted coaxially into an outer cylinder of larger radius containing water. The outer cylinder is caused to rotate by mounting it upon a turntable constructed from a commercial phonograph, and then the torque exerted hydrodynamically on the inner cylinder may be calculated from the conventional formulas of three dimensional Couette viscometry plus the known bulk phase viscosity of the water.

The disk-ring assembly is mounted over a Langmuir film balance whose trough has been machined from a solid block of teflon. The depth of the Langmuir trough is about 0.5 cm except under the area in which the ring and the disk make contact with the surface, and here a well about 4 cm deep has been drilled into the floor of the trough. The trough itself is mounted upon a tank through which water is circulated from an external thermostat, and wind currents and evaporation losses are minimized by enclosing the trough in a glove box. External mechanical vibrations are eliminated by placing the glove box upon a solid concrete block. It is a matter of some disappointment to us that we are at the present time unable to report a more successful experimental program.

References

1. G. L. Gaines, Jr., Insoluble Monolayers at Liquid-Gas Interfaces, Interscience, New York (1966), pages 89-105.
2. Ibid, pages 91-96.
3. W. D. Harkins and J. G. Kirkwood, J. Chem. Phys. 6, 53, 298 (1938).
4. F. C. Goodrich, Proc. Roy. Soc. A310, 359 (1969).
5. F. B. Hildebrand, Introduction to Numerical Analysis, McGraw-Hill, Inc. (1956), pages 389-91.
6. M. Joly, Kolloid Zeits. 126, 35 (1952).
   D. W. Deamer, D. G. Cornwell, Biophys. Biochim. Acta 116, 555 (1966).

APPENDIX I

Tables of Variation Coefficients, c_n, for Selected Values of $\lambda = \eta/\mu a$

n	λ= 0.001	λ= 0.0015	λ= 0.005	λ= 0.010	λ= 0.02	λ= 0.05	λ= 0.10	λ= 0.20	λ= 0.50	λ= 1.0	λ= 2.0
1	0.16869	0.31945	0.02495	0.04054	0.13785	0.40716	0.64343	0.82355	0.98359	1.04867	1.08402
2	1.64917	1.11674	1.82120	1.98941	1.96437	1.52039	1.04286	0.59783	0.27618	0.14558	0.07482
3	-1.37144	-1.17128	1.05689	0.42385	-0.11064	-0.42066	-0.41793	-0.18640	-0.17887	-0.17579	-0.17447
4	5.53394	7.85484	-4.84232	-4.16153	-3.34572	-2.16302	-1.37615	-0.88604	-0.40619	-0.21392	-0.10994
5	-14.68252	-20.36193	3.52846	3.62350	3.52189	2.72653	1.90004	0.89500	0.46097	0.29200	0.20246
6	12.01649	16.26212	0.81818	0.15187	-0.45281	-0.69547	-0.56558	0.04540	0.03148	0.01960	0.01100
7	17.18995	23.04062	-0.43779	-0.61537	-0.88112	-0.87906	-0.67778	-0.05532	-0.05582	-0.06463	-0.07205
8	-56.57734	-75.54547	-5.54700	-3.68396	-1.40747	0.24472	0.51750	-1.33025	-0.66506	-0.36464	-0.19172
9	68.84043	91.80333	9.56601	6.90092	3.62398	0.92405	0.15983	2.26277	1.14485	0.65287	0.37333
10	-39.06967	-51.57741	-7.39218	-5.33546	-3.00285	-1.00872	-0.35233	-1.48377	-0.72021	-0.38986	-0.20355
11	-7.37482	-11.45170	3.55860	2.40397	1.60009	0.85660	0.48476	0.15998	0.03107	-0.01249	-0.03414
12	35.66576	50.02209	-3.03357	-2.08916	-1.86947	-1.47536	-1.03755	0.17381	0.12124	0.07374	0.04077
13	-36.76172	-51.69324	4.45393	3.20526	2.70959	1.99942	1.37907	0.16212	0.05900	0.04392	0.04297
14	25.43686	36.80324	-4.56762	-3.07432	-2.30780	-1.51397	-0.98760	-0.10604	-0.01376	0.00072	0.00264
15	-16.18739	-24.70390	3.76805	2.26368	1.47702	0.83588	0.50111	-0.14473	-0.12352	-0.09236	-0.06980
16	12.22498	18.97314	-3.82626	-2.42415	-1.61880	-0.92776	-0.56848	-0.20659	-0.05836	-0.02286	-0.00954
17	-11.28842	-17.22042	4.23180	2.87506	2.01568	1.20341	0.75798	0.76106	0.32100	0.17598	0.10513
18	11.11585	17.72355	-3.85099	-2.37989	-1.54314	-0.85800	-0.51868	-0.42242	-0.11318	-0.04241	-0.01699
19	-9.98301	-17.11473	3.28277	1.72247	0.94068	0.43063	0.22892	-0.66224	-0.43364	-0.26711	-0.15874
20	7.81499	13.24238	-3.31592	-1.96290	-1.20592	-0.63187	-0.37151	1.13434	0.61944	0.34779	0.18480
21	-6.47134	-10.14287	3.44099	2.31642	1.57561	0.90466	0.55947				
22	6.59560	11.92834	-3.31116	-1.89366	-1.11421	-0.55553	-0.31882				
23	-6.38008	-14.21058	3.38891	1.50164	0.62148	0.16710	0.05051				
24	5.02864	10.83454	-3.49449	-1.88131	-1.02675	-0.46651	-0.25503				
25	-4.13656	-6.71671	3.35252	2.25275	1.50220	0.83763	0.50925				
26	4.01765	12.82310	-4.70678	-2.35550	-1.17391	-0.46967	-0.23784				
27	-2.46936	-28.01685	9.39003	3.66479	1.18092	0.08342	0.09119				
28	-0.91316	36.96337	-14.80048	-6.51818	-2.77455	-0.84294	-0.34020				
29	3.04235	-29.48920	15.27876	8.14539	4.54922	2.14491	1.19754				
30	-2.06376	13.04156	-9.29019	-5.97187	-3.97238	-2.20610	-1.31688				

APPENDIX II

Interpolation Polynomial Coefficients b_n for the Calculation of Film Torque. See Equations (9) and (10).

n	$0 \leq \lambda < 0.10$	$0.10 \leq \lambda < 1.0$	$1.0 \leq \lambda$
0	0.84012	0.69868	-
1	-6.9498	-0.000043	-0.44681
2	76.254	0.00080	0.00022
3	0.0	-0.04894	0.10154
4	-2380.3	-	-

APPENDIX III

Torque Table for the Rotating Disk μ= substrate viscosity (g $sec^{-1} cm^{-1}$); ω = angular velocity of the disk (sec^{-1}); a = radius of the disk (cm); η= surface viscosity (g sec^{-1}). All torque entries are in units $\omega\mu a^3$.

$\lambda = \mu / \mu a$	Film torque	Substrate torque	Total torque	Excess torque
0	0	5.333 = 16/3	5.333	0
.005	0.582	4.621	5.203	-0.131
.010	0.870	4.407	5.278	-0.056
.015	1.117	4.245	5.362	+0.029
.020	1.341	4.114	5.455	0.122
.030	1.747	3.910	5.657	0.323
.040	2.105	3.757	5.862	0.529
.050	2.416	3.638	6.054	0.721
.060	2.685	3.543	6.228	0.895
.080	3.137	3.400	6.536	1.203
.100	3.540	3.296	6.836	1.503
.200	5.280	3.093	8.374	3.040
.300	6.820	2.977	9.797	4.464
.500	9.555	2.865	12.420	7.087
.800	13.363	2.797	16.160	10.827
1.000	15.942	2.773	18.715	13.382

Figure 1. Interfacial Velocity Profiles v for the Rotating Disk.

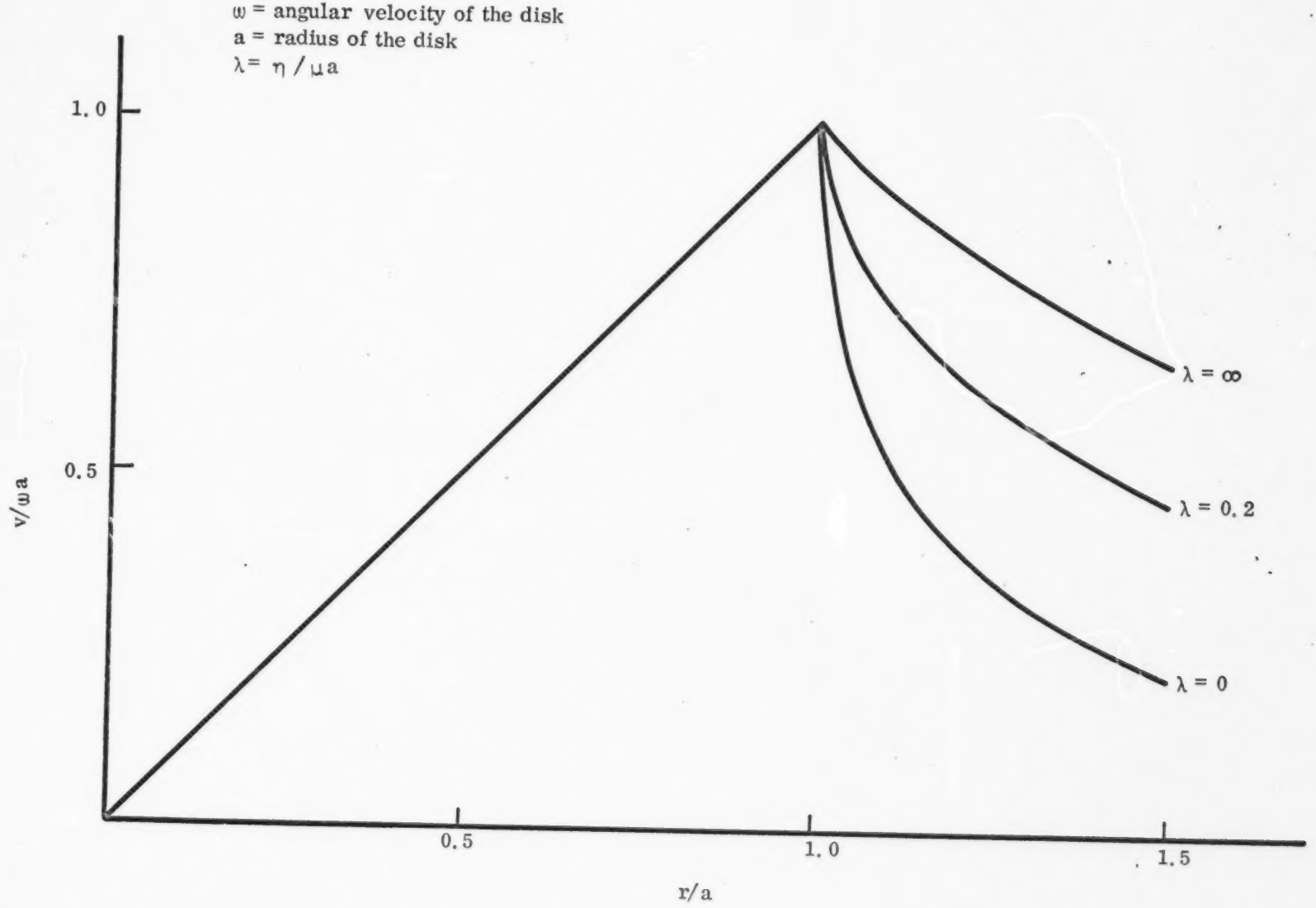

Figure 2. Film Torque Exerted on the Rotating Disk.

A = Exact

B = "Naive" approximation

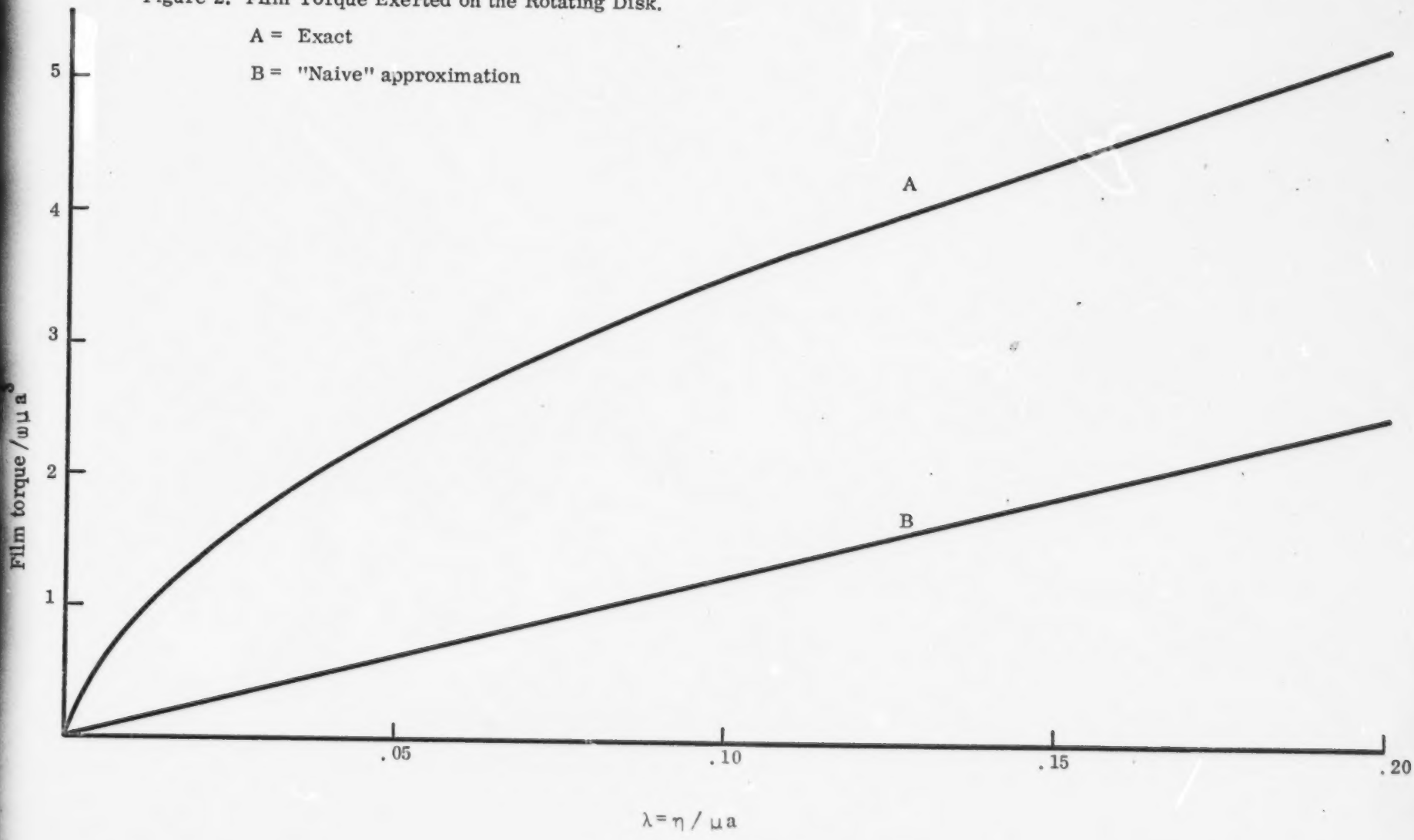

hc

Figure 3. Substrate Torque Exerted on the Rotating Disk.

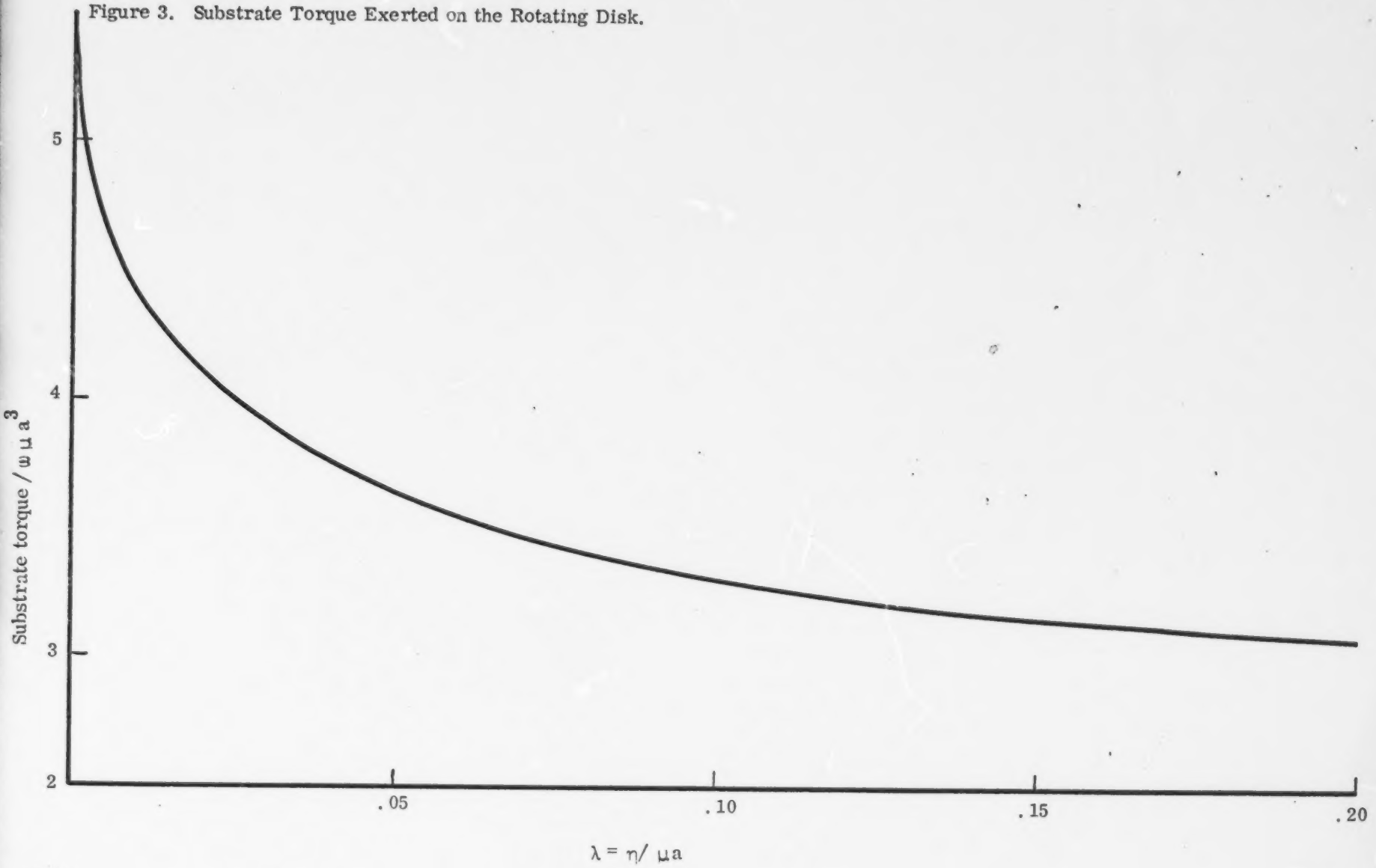

Figure 4. Excess Torque Exerted on the Rotating Disk

A = Exact

B = "Naive" approximation

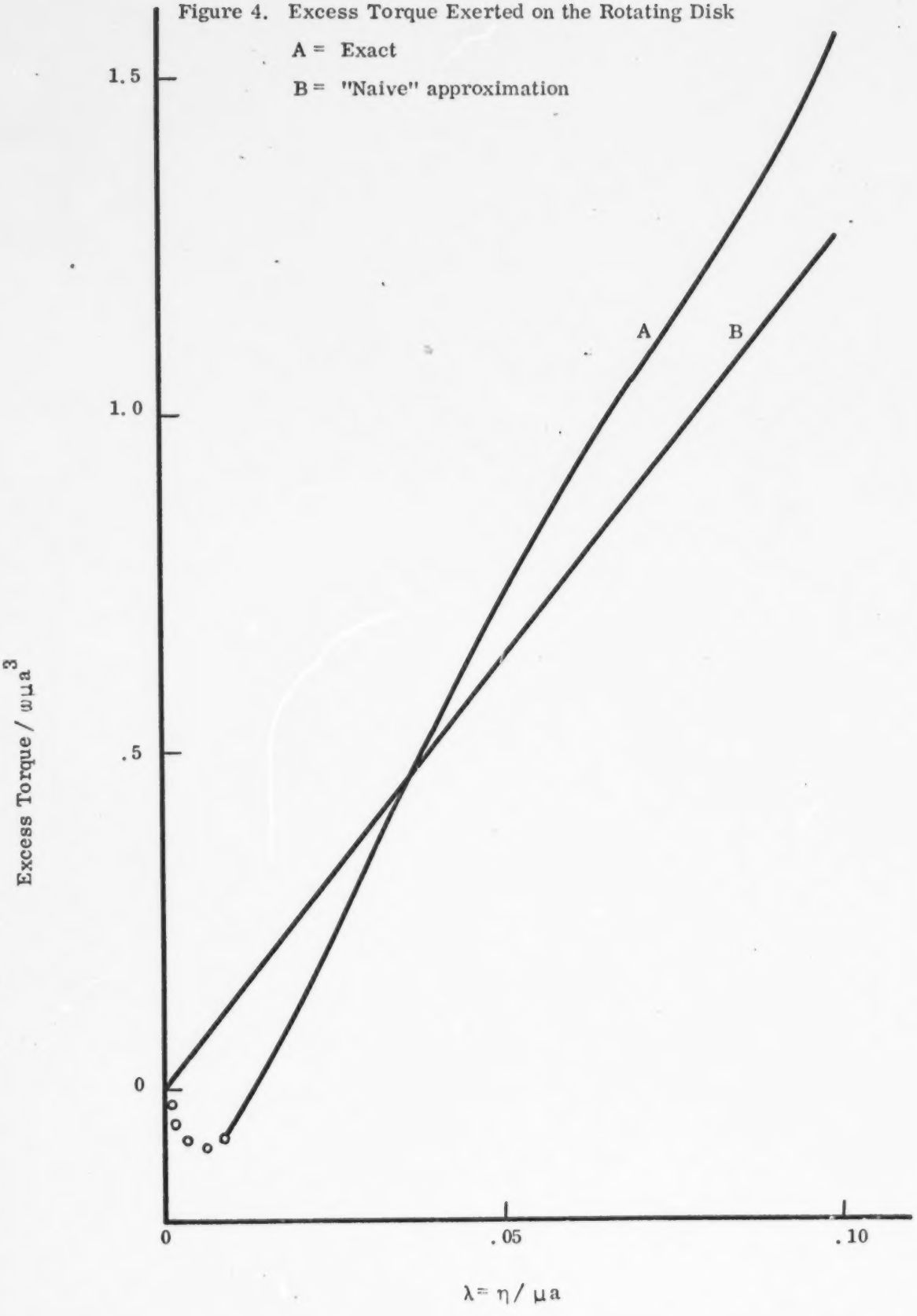

Figure 5. A Disk-Ring Interfacial Velocity Profile

Ring Radius = 3 a; $\lambda = \eta / \mu a = 0.1$

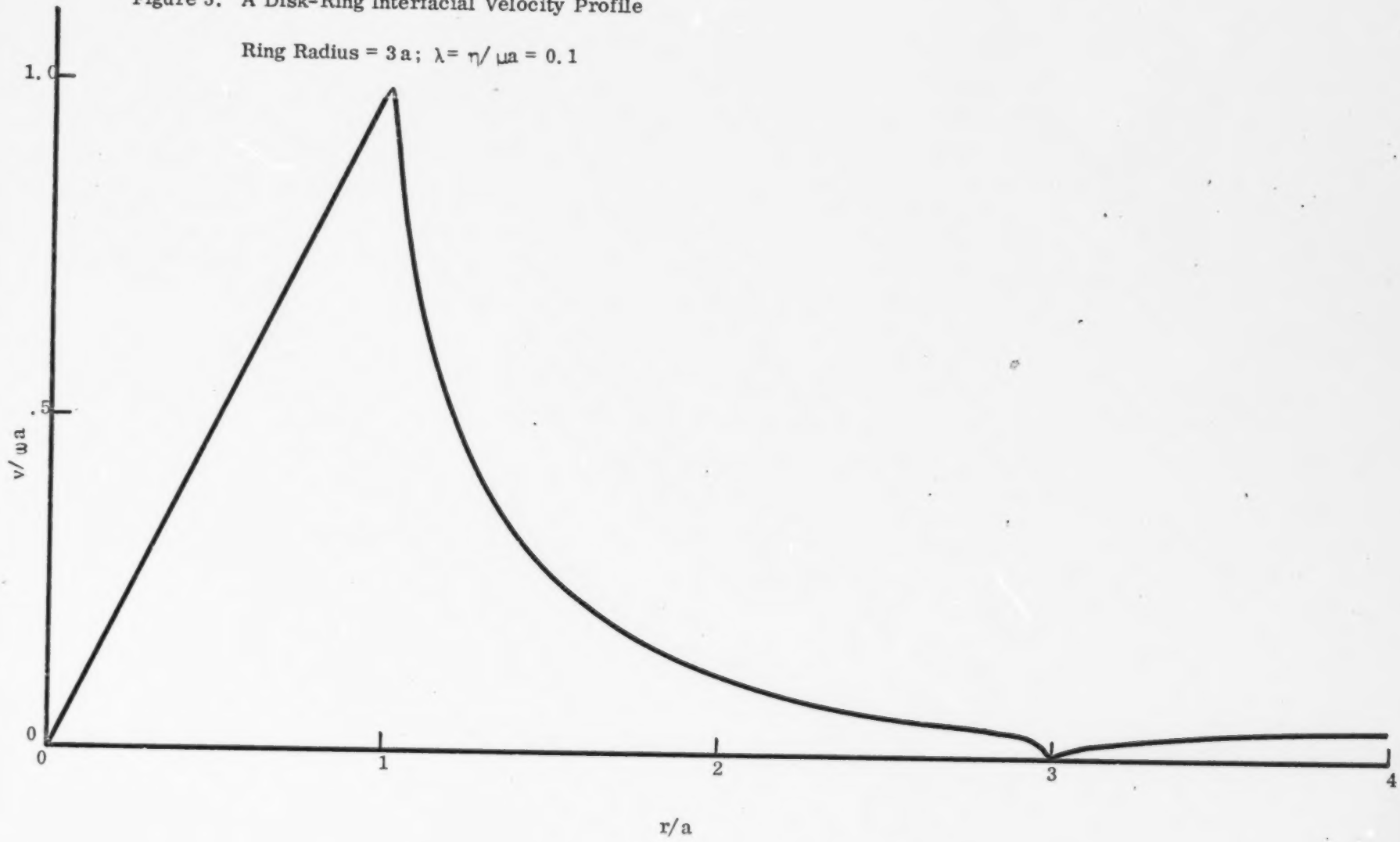

27

Figure 6

THE COUETTE SURFACE VISCOMETER

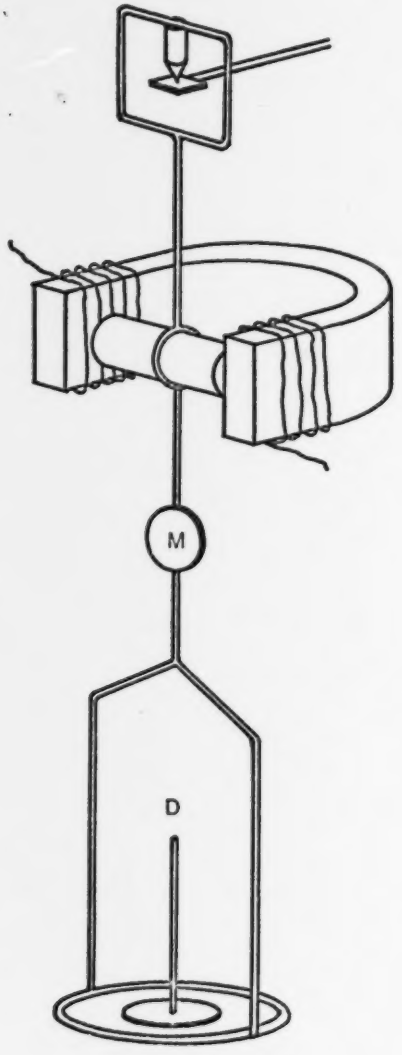

M = galvanometer mirror

D = rotating disk